BIOCHEMISTRY
including biophysical chemistry & molecular biology

Article

pubs.acs.org/biochemistry

The N-Terminal Extension of βB1-Crystallin Chaperones β-Crystallin Folding and Cooperates with αA-Crystallin

Xiao-Yao Leng,[#] Sha Wang,[#] Ni-Qian Cao, Liang-Bo Qi, and Yong-Bin Yan*

State Key Laboratory of Biomembrane and Membrane Biotechnology, School of Life Sciences, Tsinghua University, Beijing 100084, China

ABSTRACT: β/γ-Crystallins are the major structural proteins in mammalian lens. The N-terminal truncation of βB1-crystallin has been associated with the regulation of β-crystallin size distributions in human lens. Herein we studied the roles of βB1 N-terminal extension in protein structure and folding by constructing five N-terminal truncated forms. The truncations did not affect the secondary and tertiary structures of the main body as well as stability against denaturation. Truncations with more than 28 residues off the N-terminus promoted the dissociation of the dimeric βB1 into monomers in diluted solutions. Interestingly, the N-terminal extension facilitated βB1 to adopt the correct folding pathway, while truncated proteins were prone to undergo the misfolding/aggregation pathway during kinetic refolding. The N-terminal extension of βB1 acted as an intramolecular chaperone (IMC) to regulate the kinetic partitioning between folding and misfolding. The IMC function of the N-terminal extension was also critical to the correct refolding of β-crystallin heteromer and the action of the lens-specific molecular chaperone αA-crystallin. The cooperation between IMC and molecular chaperones produced a much stronger chaperoning effect than if they acted separately. To our knowledge, this is the first report showing the cooperation between IMC and molecular chaperones.

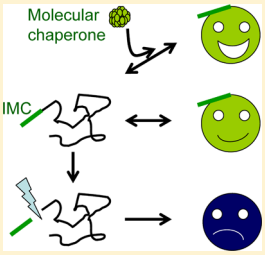

In mature mammalian lens fiber cells, the intracellular organelles are degraded in an apoptotic-like manner to minimize light scattering during the transmission of visible light through the lens.[1] As a result, there is little or no protein turnover in mature lens fiber cells, and the lens proteins are required to maintain stability across an individual's lifespan.[2−4] Crystallins, which are the dominant structural proteins in mammalian lens, are believed to be responsible for the maintenance of the transparency and refractive index of the lens.[5,6] Aggregation of crystallins and/or their proteolytic fragments caused by aging or inherited mutations has been linked to the onset of cataract, which is the opacification of the lens leading to loss of vision.[7,8] The importance of crystallins in lens transparency has been evidenced by the discovery of numerous inherited mutations associated with autosomal dominant congenital cataract.[9]

The mammalian crystallins are categorized into three classes (α, β, and γ) based on their elution positions on the size-exclusion chromatography (SEC) profile. In diluted solutions, they are distinct in their oligomerization states: α-crystallin with an average of ∼24 subunits, β-crystallin with 2−8 subunits, and γ-crystallin existing as a monomer.[2,3] The β- and γ-crystallins, which form the β/γ-crystallin family, share a conserved tertiary structure with four Greek-key motifs divided into two domains (Figure 1).[3] There are seven members in human β-crystallins: four acidic (βA1, βA2, βA3, βA4) and three basic forms (βB1, βB2, and βB3). β-Crystallins can exist as homomers or heteromers in the lens, and heteromers are generally formed between acidic and basic β-crystallins.[10,11] The structural basis for the oligomerization-prone property of β-crystallins remains elusive, although many previous papers have addressed this problem in the last ∼30 years.[10−23] Nonetheless, it is clear that the extra N- and C-terminal extensions of β-crystallins play an important role in the homo- and hetero-oligomerization of β-crystallins.[11,13,14,17,21,24−28] Among the seven β-crystallins, βB1 is unique for the longest N- and C-terminal extensions (Figure 1A). NMR and biophysical studies have shown that the N-terminal extension of βB1 is dominated by unordered structures,[18,26,29] and residues 29−47 are proposed to form helical structures adjacent to the main body of the molecule.[26] The loop from residues 48 to 56 is thought to be crucial to the homo- and hetero-oligomerization of βB1.[19,26,27]

During lens development and aging, β-crystallins are found to have various post-translational modifications including the truncations of the N- and C-terminal extensions.[4,16,30−33] Extensive fragmentation and proteolysis of crystallins are associated with age-related cataract[4,32,33] and congenital cataract.[34] However, the truncations of the N-terminal extensions of βB1 and βA3 may occur early during lens development since the truncated forms are detected even in newborns.[30,31] This suggests that the N-terminal extensions of these two proteins may play a role in lens development, although the underlying mechanism is unclear. The length of βB1 N-terminal extension is found to correlate with the size distribution of β-crystallin oligomers in the lens.[16] However, the N-terminal truncations ranging from 15 to 41 residues have been identified in the soluble fraction of normal human lens.[16,30,31,35] Consistently, the truncations with the removal of 41 or 47 residues at the N-terminus are found to have no impact on βB1 stability against thermal aggregation or urea-

Received: February 3, 2014
Revised: March 25, 2014
Published: March 26, 2014

dx.doi.org/10.1021/bi500146d | *Biochemistry* 2014, 53, 2464−2473

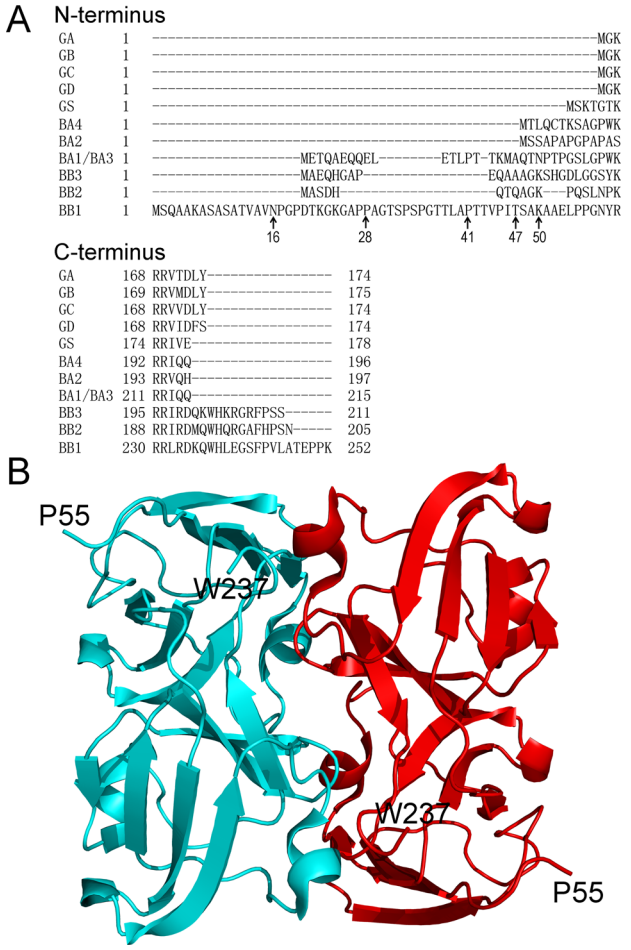

Figure 1. Sequence alignment of β/γ-crystallins and crystal structure of truncated βB1. (A) Sequence alignment of the N- and C-termini of human β/γ-crystallins. The positions of the sites for various truncated mutants constructed in this research are indicated by arrows. (B) Crystal structure of the truncated βB1 (PDB ID: 1OKI). The residues at the N- and C-termini are labeled. The residues are numbered by taking Met as 1. The two subunits of the dimeric βB1 are colored in red and cyan, respectively.

induced denaturation.[29,36] Thus, it remains to be elucidated as to why βB1 has an evolutionary conserved long N-terminal extension that is cleaved after translation. To further investigate the role of the N-terminal extension of βB1, we studied the properties of mutants with the removal of 16, 28, 41, 47, or 50 residues off the N-terminus (βB1Δ16, βB1Δ28, βB1Δ41, βB1Δ47, and βB1Δ50, respectively), which mimicks the proteolytic sites either in human lens or in vitro and the disruption of the critical region for homo- or hetero-oligomerization identified previously. A detailed comparison of the biophysical properties confirmed previous findings that the N-terminal extension contributed little to the stability of the homomers and heteromers. The N-terminal extension significantly affected the kinetic partitioning between the correct refolding and misfolding/aggregation pathways. We proposed that the N-terminal extension acted as an intramolecular chaperone (IMC) to facilitate the folding and assembly of βB1-crystallin. More importantly, we found that there is cooperation between the actions of IMC and the molecular chaperone αA, which might be important to the understanding of the quality control mechanisms in the cells.

MATERIALS AND METHODS

Reagents. The Taq polymerase and the restriction endonucleases *Bam*HI and *Hin*dIII were from Takara. Ultrapure guanidine hydrochloride (GdnHCl), isopropyl-1-thio-β-D-galactopyranoside (IPTG), sodium dodecyl sulfate (SDS), 1-anilinonaphtalene-8-sulfonate (ANS), dithiothreitol (DTT), acrylamide and bovine serum albumin were obtained from Sigma. Kanamycin was purchased from Amresco. All other reagents were local products of analytical grade.

Preparation of Protein Samples. The cloning of the genes of the wild type (WT) αA, βB1, and βA3 has been described previously.[37,38] The mutants βB1Δ16, βB1Δ28, βB1Δ41, βB1Δ47, and βB1Δ50 (amino acid residues are numbered starting at Met1) were obtained by the standard site-directed mutagenesis procedures using the following forward primers: βB1Δ16-F: 5′-CGGGATCCATGCCAGGGCCT-GACACC-3′, βB1Δ28-F: 5′-CGGGATCCATGGCAGGAAC-ATCCCCTA-3′, βB1Δ41-F: 5′-CGGGATCCATGAGC-GCCAAGGCGGCG-3′, βB1Δ47-F: 5′- CGGGATCCAT-GAGCGCCAAGGCGGCG-3′ and βB1Δ50-F: 5′-CGGGATCCATGGCGGCGGAACTGCCT-3′. The reverse primer for the five mutants was 5′-CCCAAGCTTTCACTT-GGGGGGCTCTGTG-3′. The recombinant WT and mutated β-crystallin proteins were overexpressed in *Escherichia coli* Rosetta and purified by Ni-NTA affinity column followed by gel filtration chromatography using the same protocol as those described elsewhere.[38] We also prepared βB1Δ50 by removing the His-tag and the first 50 residues by the digestion of trypsin. A comparison between the proteins with and without His-tag indicated that the existence of His-tag did not affect the biophysical properties and refolding behavior of β-crystallins (data not shown). The purification of the recombinant αA-crystallin was performed as described previously.[39] The final protein products were homogeneous on 12.5% SDS-PAGE and eluted as a single peak in the size-exclusion chromatography (SEC) profile. The SEC analysis of the samples was carried out on a Superdex 75 HR 10/30 column equipped on an ÄKTA FPLC (Amersham Pharmacia Biotech, Sweden) as described previously.[38] The protein concentration was determined according to the Bradford method.[40] The βB1/βA3 heteromer was prepared by incubating an equivalent molar amount of βB1 and βA3 at 37 °C for 4 h and checking by SEC analysis. All protein samples were prepared in buffer A containing 20 mM sodium phosphate, 150 mM NaCl, 1 mM EDTA, and 1 mM DTT. For simplicity, the protein molar concentration was calculated by assuming that all proteins were in the monomeric states (the molar concentration of the subunits).

Spectroscopic Experiments. Details regarding the spectroscopic experiments were the same as those described elsewhere.[23,34] In brief, the spectroscopic experiments were performed at 25 °C using samples with a protein concentration of 6.9 μM in buffer A unless mentioned otherwise. The fluorescence emission spectra were measured on a Hitachi F-2500 spectrofluorimeter using a 200 μL curvette and a resolution of 0.5 nm. The intrinsic Trp fluorescence was excited at 295 nm, while the ANS extrinsic fluorescence was excited at 380 nm. Parameter A, which is a sensitive monitor of the shape and position of the Trp fluorescence spectrum, was obtained by dividing the fluorescence intensity at 320 nm by that at 365 nm.[41] Resonance light scattering, which can detect small aggregates that are invisible by turbidity measurements, was performed using the same method as described previously

dx.doi.org/10.1021/bi500146d | *Biochemistry* 2014, 53, 2464−2473

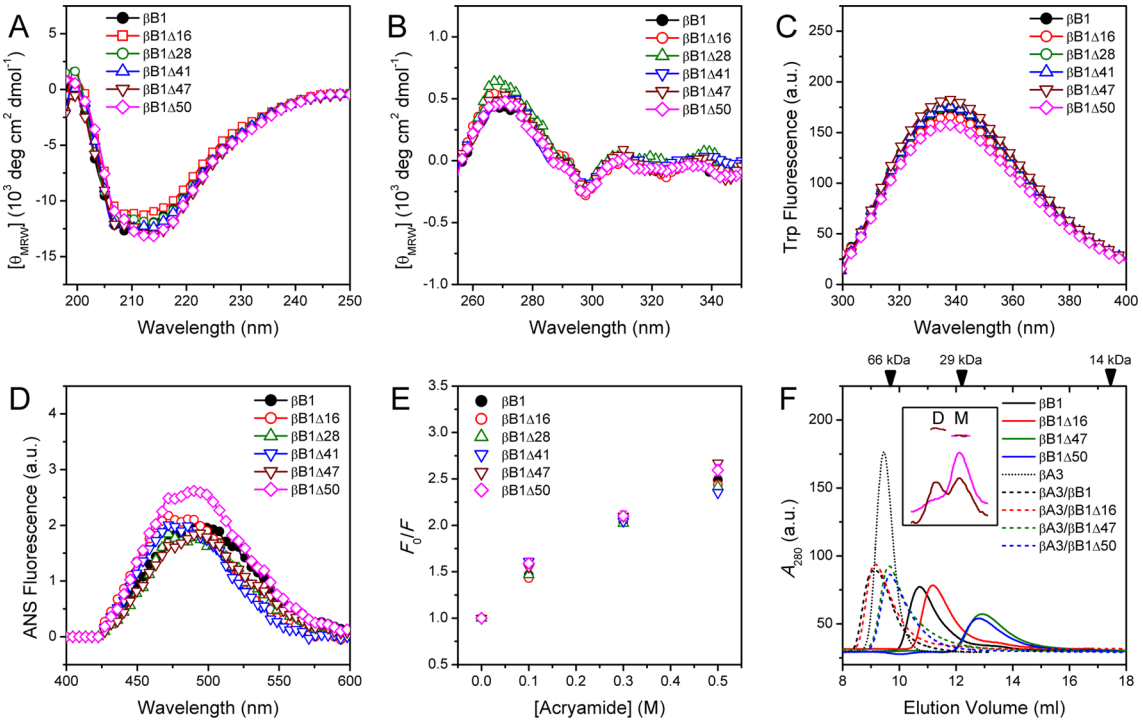

Figure 2. Effects of the N-terminal truncations on βB1 structure and assembly. (A) Far-UV CD. (B) Near-UV CD. (C) Intrinsic Trp fluorescence with an excitation wavelength of 295 nm. (D) Extrinsic ANS fluorescence with an excitation wavelength of 380 nm. (E) Trp fluorescence quenching by acryamide. (F) SEC analysis. The inset of panel F shows the SLS analysis of βB1 and βB1Δ50. The behavior of βB1Δ16 was the same as that of βB1, while those of βB1Δ28, βB1Δ41, and βB1Δ47 were the same as that of βB1Δ50 (data not shown). The protein samples were prepared in buffer A containing 20 mM sodium phosphate, 150 mM NaCl, 1 mM EDTA, and 1 mM DTT. The presented spectra were obtained by subtracting the original spectra by that of the control. The control spectra of CD and Trp fluorescence were measured using buffer A, while that of ANS fluorescence was measured using buffer A with the addition of 75 mM ANS. The protein concentration was 6.9 μM for far-UV CD, Trp and ANS fluorescence measurements and 34.5 μM for near-UV CD and SLS analysis.

by exciting at 295 nm and recording at 90° on a Hitachi F-2500 spectrofluorimeter.[42] The circular dichroism (CD) spectra were recorded on a Jasco-715 spectrophotometer. Far-UV CD was measured using a 0.1 cm-path length cell and a protein concentration of 3.45 μM, while the near-UV CD was measured using a 1-cm path length cell and a protein concentration of 34.5 μM. Static light scattering (SLS) experiments were performed by separating the proteins with a concentration of 34.5 μM using a size exclusion chromatography column for multi-angle light scattering purchased from Wyatt Technology (WTC-030S5). Fluorescence quenching by acrylamide was performed using the same procedure as that described elsewhere.[43] In brief, the proteins were incubated for 2 h in buffer A with or without the addition of 0.1, 0.3, or 0.5 M acrylamide at room temperature. The quenching effect of acrylamide (F_0/F) was obtained by dividing the Trp fluorescence intensity at 340 nm of the sample in the absence of acrylamide (F_0) by that of the sample with the addition of acrylamide (F).

Protein Stability. The thermal stability of the proteins was evaluated by heating the protein samples continuously with the temperature increased from 30 to 86 °C. The temperature was controlled by a water bath. The far-UV CD, Trp fluorescence, light scattering, or turbidity data were recorded every 2 °C after 2 min equilibration. The stability against chemical denaturants GdnHCl was measured by denaturing the proteins in the buffers containing various concentrations of GdnHCl ranging from 0 to 6 M. After denaturation overnight (12−16 h), the samples were used for far-UV CD, Trp fluorescence, or turbidity experiments. The protein concentration was 0.2 mg/mL (~6.9 μM).

Protein Thermal Aggregation. Protein aggregation was monitored by turbidity (absorbance at 400 nm) recorded on an Ultraspec 4300 pro UV/visible spectrophotometer from Amersham Pharmacia Biotech (Uppsala, Sweden). The temperature dependence of aggregation was measured after the samples were equilibrated at a given temperature for 2 min. The thermal aggregation kinetics was determined by recording the turbidity immediately after the proteins were heated at 75 °C. The final protein concentration was 0.2 mg/mL for protein thermal aggregation experiments.

Protein Aggregation during Refolding. The proteins were fully denatured in 4 M GdnHCl at 25 °C for 4 h. The refolding was initiated by a 1:40 manual fast dilution of the GdnHCl-denatured proteins in the refolding buffer (buffer A containing 20 mM sodium phosphate, 150 mM NaCl, 1 mM EDTA, and 1 mM DTT). The final protein concentration for the refolding experiments was 3.45 μM. The effects of β- and αA-crystallins were evaluated by refolding the denatured proteins in buffer A with the addition of equal molar amount of native β- or αA-crystallins. The co-refolding of βA3/βB1 was performed by kinetic refolding of the denatured βA3/βB1 heteromer as described previously.[23] The effect of the synthetic peptide corresponding to first 50 residues of βB1 was evaluated by refolding of the denatured β-crystallins in buffer A in the presence or absence of the synthetic peptide with a molar ratio of [protein]/[peptide] = 1:60. The time-course aggregation during refolding was monitored by turbidity, and the data were

dx.doi.org/10.1021/bi500146d | Biochemistry 2014, 53, 2464−2473

recorded every 2 s for 10−20 min. After refolding for 60 min, the samples were centrifuged at 12 000 rpm for 8 min to separate the soluble and insoluble fractions. The insoluble precipitations were washed twice using the refolding buffer, and the precipitations were resuspended in 400 μL of refolding buffer. Then the soluble and insoluble fractions were analyzed by 12.5% SDS-PAGE.

RESULTS

Effects of the N-Terminal Truncation on βB1-Crystallin Structure and Assembly. Previous studies have shown that the removal of 56 or 59 residues off the N-terminus results in completely insoluble overexpression of βB1 in *E. coli* BL21 cells.[26,27] In this research, the overexpressed recombinant proteins of shorter truncations (βB1Δ16, βB1Δ28, βB1Δ41, βB1Δ47, and βB1Δ50) were found to exist in both the soluble and insoluble fractions. The structural features of the purified proteins were investigated via biophysical methods. As shown in Figure 2A, the CD spectrum of βB1 contained a negative peak centered at ∼213 nm and an obvious shoulder at around 207 nm, which is consistent with the previous observations.[26,27,36,38] The N-terminal truncations altered the shape of the CD spectrum of βB1 with a significant decrease of the shoulder peak at ∼206 nm. Thus, the truncated mutants contained more ordered β-sheet components, which coincided with the proposal that the N-terminal extension of βB1 is dominated by unordered flexible structures as well as potential helical structures[18,26,29] and the crystal structure of the truncated βB1 (Figure 1B). No significant changes were observed for the tertiary structure of βB1 by the truncations as reflected by the almost superimposed data of near-UV CD (Figure 2B), the emission maximum wavelength (E_{max}) of the Trp fluorescence (Figure 2C), the ANS fluorescence (Figure 2D), and the fluorescence quenching by acrylamide (Figure 2E). A slight increase (∼25%) could be seen for βB1Δ50, which might be caused by the exposure of adjacent hydrophobic sites around Arg50 since neither the core structure (Figure 2C,E) nor the stability (see below) was altered by the truncation.

The alteration in βB1 quaternary structure was studied by the SEC method for three truncated mutants, βB1Δ16, βB1Δ47, and βB1Δ50 (Figure 2F). Consistent with the previous observations,[10] βB1 eluted at a position between the monomeric and dimeric molecules. When separated by the column used for SLS at a protein concentration of 34.5 μM (1 mg/mL), βB1 contained two almost identical peaks corresponding to the dimeric and monomeric forms (inset of Figure 2F). At a higher concentration of 5 mg/mL, the dimeric peak was the dominant one.[38] These observations were consistent with the previous studies showing that that β-crystallins exist in a dimer−monomer equilibrium at low protein concentrations.[10,21,34,44] The behavior of βB1Δ16 in SLS analysis was similar to βB1 (data not shown) and had a 0.4 mL larger elution volume in the SEC profile, which might be caused by the smaller molecular weight and the lack of the flexible N-terminus. However, βB1Δ47 and βB1Δ50 were eluted at a position close to the molecular weight of monomers. SLS analysis indicated that βB1Δ28, βB1Δ41, βB1Δ47, and βB1Δ50 mainly existed in the monomeric state with a small fraction of dimer, which is consistent with the previous observation of the truncated βB1 with the removal of 47 residues off the N-terminus and five residues off the C-terminus.[44] Although the removal of 47 or 50 residues from the N-terminus significantly shifted the dimer−monomer equilibrium of βB1, it did not affect the association of βB1 with βA3 as evidenced by the single peak in the SEC elution profiles and dynamic light scattering measurements of the heteromers (data not shown).

The N-Terminal Extension Contributes Little to βB1-Crystallin Stability. Early studies have shown that the removal of 41 residues from the N-terminus does not affect βB1 stability against urea-induced unfolding,[36] and the truncated form generated by calpain cleavage has thermal aggregation properties similar to the WT protein.[29] We performed a comprehensive comparison of the stabilities against heat and GdnHCl between the WT βB1 and the truncated mutants βB1Δ16, βB1Δ47, and βB1Δ50 via biospectroscopic techniques. A summary of the midpoints of the transitions (T_m) probed by various methods is shown in Figure 3A. Our results showed that truncations up to 50 residues off the N-terminus did not affect the thermal denaturation of βB1 when monitored by CD (secondary structure), Trp fluorescence (tertiary structure), light scattering (oligomerization and aggregation), or turbidity (amorphous aggregation). The truncated mutants had almost superimposed transition curves during GdnHCl-induced denaturation (Figure 3B). Similarly, no significant effects of the truncations were observed for the thermal denaturation of the βA3/βB1 heteromers (data not shown).

The N-Terminal Extension Is Crucial to βB1-Crystallin Refolding. The aggregation kinetics during refolding was monitored immediately after the fast manual mixing of the GdnHCl-denatured proteins with the refolding buffer (Figure 4). As the controls, βB1 did not aggregate during kinetic refolding, while βA3 aggregated immediately after mixing, consistent with our previous observations although different refolding conditions were applied.[23] The behavior of βB1Δ16 was the same as that of the WT protein, while longer truncations significantly promoted βB1 aggregation during refolding. SDS-PAGE analysis of the samples refolded for 1 h after mixing indicated that unlike the fully reversible refolding of βB1 and βB1Δ16, almost all of the βB1Δ28, βB1Δ41, βB1Δ47, and βB1Δ50 molecules were found in the precipitations. A small fraction of βB1Δ28 could also be detected in the soluble fraction in the SDS-PAGE gel. It is worth noting that the maximum value of the turbidity was not always linearly correlated to the amounts of aggregates characterized by SDS-PAGE, which might be caused by the different incubation times and/or the fact that turbidity reflects both the amount and size of the aggregates.[45,46] Nonetheless, these observations suggested that the existence of the N-terminal extension from residues 17 to 28 could successfully prevent βB1 being trapped in the misfolding and aggregation pathway, while the kinetic partitioning between folding and misfolding could be altered to favor misfolding by the removal of ≥28 residues off the N-terminus.

The N-terminal Extension of βB1-Crystallin Is Necessary for Assisting βA3-Crystallin Refolding. The folding of βA3 has been shown to be irreversible and is prone to undergo the misfolding/aggregation pathway during refolding, while βB1 can assist βA3 folding by the formation of heteromers during co-refolding.[23] Although the N-terminal truncations affected βB1 quaternary structure, the mutants still possessed the ability to form stable heteromers with βA3 (Figure 2F). The existence of native βB1 and various mutants in the refolding buffer has no impact on the refolding of βA3 (Figure

dx.doi.org/10.1021/bi500146d | Biochemistry 2014, 53, 2464−2473

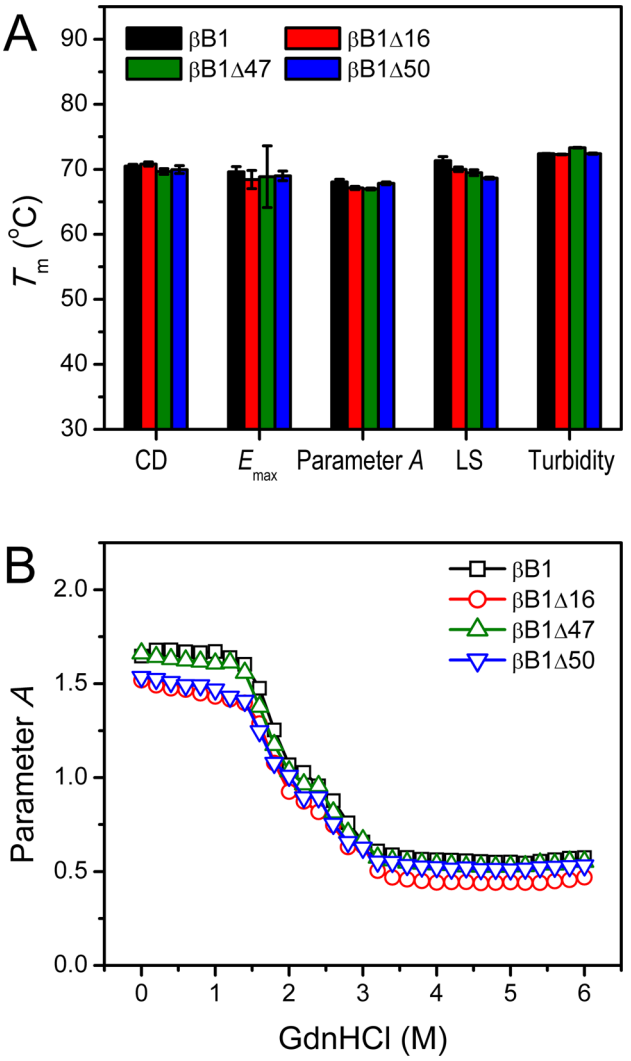

Figure 3. Effect of the N-terminal truncations on βB1 stability against heat- and GdnHCl-induced denaturation. (A) The midpoints of βB1 thermal transitions (T_m) measured by the ellipticity at 215 nm of the CD spectra, the emission maximum wavelength of the Trp fluorescence (E_{max}), parameter *A* obtained by dividing the Trp fluorescence intensity at 320 nm by that at 365 nm, Rayleigh resonance light scattering excited at 295 nm and turbidity determined by the absorbance at 400 nm, from left to right, respectively. (B) The transition curves of the proteins during GdnHCl-induced denaturation reflected by parameter *A*.

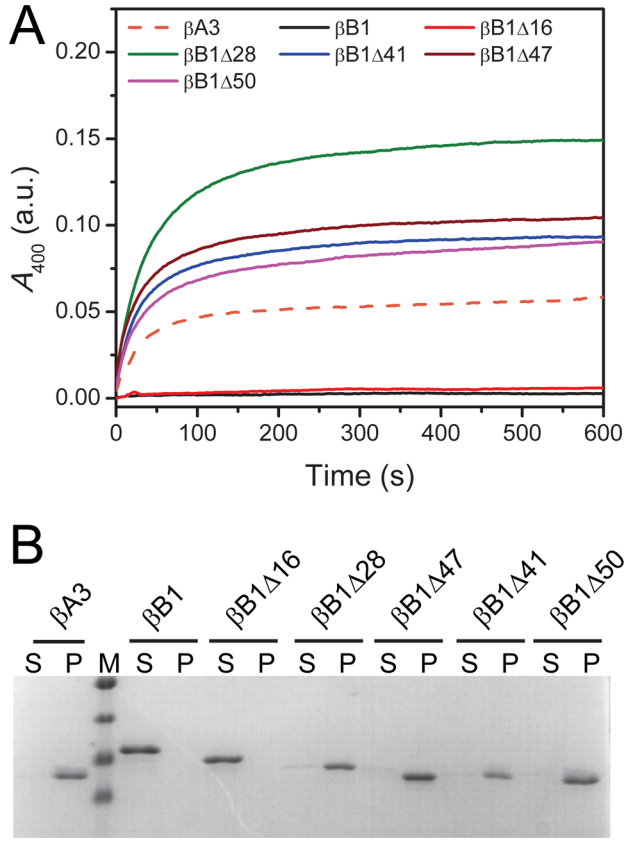

Figure 4. Effect of the N-terminal truncations on the kinetic partitioning between folding and misfolding/aggregation pathways of βB1 during refolding from the GdnHCl-denatured states. (A) Aggregation kinetics during refolding measured by the time-course changes of the turbidity. The proteins were denatured in 4 M GdnHCl for 4 h at 25 °C. The turbidity data were recorded every 2 s after the denatured proteins were diluted into buffer A with a ratio of 1:40 by fast manual mixing. (B) SDS-PAGE analysis of the samples after 60 min incubation in the refolding buffer. The supernatant (S) and precipitation (P) were separated by centrifugation. The pellets were washed twice by buffer A. The data of βA3 were also shown as a control. M is the marker and the molecular weights are 55, 43, 34, 26 kDa, from top to bottom, respectively.

5A), which might be caused by the rate of aggregation during kinetic refolding is much faster than the subunit exchange rate. In the lens, α-crystallins act as molecular chaperones to assist protein folding and avoid the occurrence of off-pathway aggregates.[47] However, the protecting effect of αA on βA3 is very weak since only a small portion of βA3 was found in the soluble fractions of the refolded samples, and some αA molecules were also codeposited into the insoluble fraction (Figure 5B). On the contrary, the aggregation of βA3 could be successfully suppressed by βB1 during co-refolding (the line and lane for βA3/βB1 in Figure 6A). The removal of 16 residues weakened, while the removal of ≥28 residues almost completely diminished, the ability of βB1 to protect βA3 during co-refolding (blue dashed lines in Figure 6).

The N-Terminal Extension Amplifies the Chaperone Function of αA-Crystallin. Although the full-length βB1 could protect βA3 against aggregation during co-refolding, there were considerable amounts of heteromers in the insoluble fractions even at a low concentration of 3.45 μM βA3/βB1 (1.725 μM βA3 + 1.725 μM βB1). Considering that the protecting effect of αA on βA3 is very weak, βA3 was a "bad" substrate for αA. On the contrary, the βA3/βB1 heteromer was a "good" substrate for αA as revealed by the complete suppression of the aggregation pathway during refolding by an equal molar amount of αA in the refolding buffer (Figure 6A). The truncated mutants behaved dissimilarly in response to the action of αA. That is, βA3/βB1Δ16 was a good substrate for αA as revealed by the efficient blocking of the aggregation pathway of βA3/βB1Δ16 by αA (Figure 6B). However, βB1Δ41, βA3/βB1Δ41 (Figure 6D), βB1Δ47, βA3/βB1Δ47, βB1Δ50, and βA3/βB1Δ50 (data not shown) were bad substrates reflected by the low efficiency of αA in preventing β-crystallin heteromer aggregation and the tethering of some of the αA molecules codeposited in the precipitation fractions. The behaviors of βB1Δ28 and βA3/βB1Δ28 were between proteins containing βB1Δ16 and βB1Δ41 as revealed by the partial aggregation-inhibiting effect of αA (Figure 6C).

dx.doi.org/10.1021/bi500146d | *Biochemistry* 2014, 53, 2464−2473

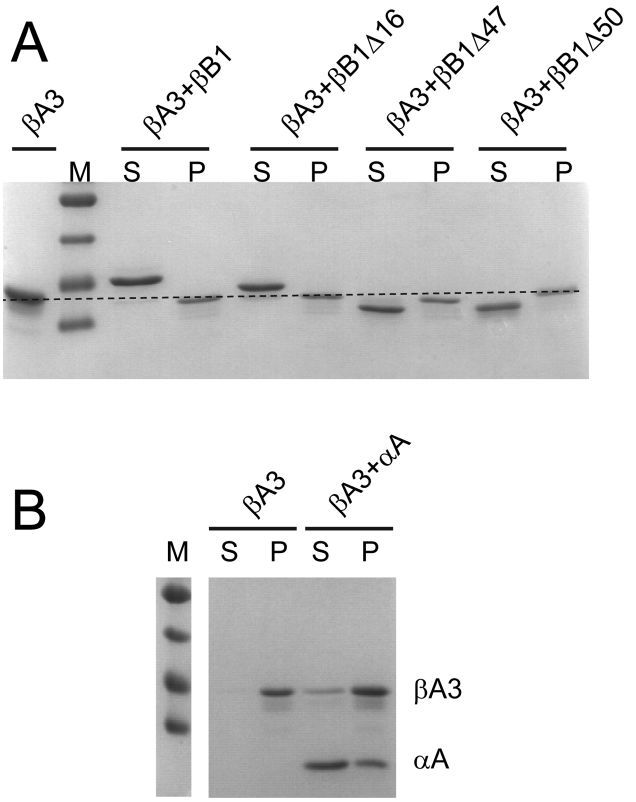

Figure 5. Effect of the well-folded βB1 and αA on βA3 aggregation during refolding. (A) SDS-PAGE analysis of βA3 aggregation during refolding in the presence or absence of the well-folded WT or truncated βB1 proteins. The positions of βA3 in the gel are indicated by the dotted line. (B) SDS-PAGE analysis of the partitioning between the folding and misfolding pathways of βA3 in the presence or absence of αA in the refolding buffer. βA3 refolding was initiated by a fast manual mixing of the 4 M GdnHCl-denatured βA3 with buffer A in the presence or absence of an equal molar amount of βB1 or αA. The experimental conditions were the same as those described in Figure 4B.

Moreover, the existence of native βA3 in the refolding buffer did not affect the aggregation behavior of the WT and truncated βB1 proteins. A close inspection of the results in Figures 4 and 6 could assign the key regions for the self-refolding of βB1 and βA3/βB1 as well as the action of αA by observing the shortest and longest N-terminal extension in βB1 that required for efficient kinetic refolding. Surprisingly, it seems that the key regions were partially overlapping but distinct: residues 17−28 for self-refolding of βB1, residues 1−28 for self-refolding of βA3/βB1, and residues 17−41 for the chaperone function of αA.

The peptide corresponding to the first 50 residues of βB1 was synthesized to further characterize the properties of the N-terminal extension of βB1. As can be seen from Figure 7, no significant effect was observed for βB1Δ50 and βA3/βB1Δ50 aggregation when the peptide was added to the refolding buffer. The peptide could partially retard βA3 aggregation. The differential effect of the peptide on βB1Δ50 and βA3 refolding might be caused by the dissimilar roles of βB1 N-terminal extension in the oligomerization of βB1 homomer and βA3/βB1 heteromer (Figure 2F). When the proteins were refolded in buffer with both the synthetic peptide and αA, the aggregation of the proteins was more serious than those in buffer with αA. At present, it is difficult to distinguish whether the antichaperone effect of the synthetic peptide on αA function was caused by the opposing effect of the covalently linked N-terminal extension of βB1 or the interference of αA function by nonspecific binding.

DISCUSSION

The terminal extensions have been known to be critical for the assembly of β-crystallins for many years (reviewed in refs 3 and 48). Truncations of less than 47 residues have been identified in the soluble fraction of the normal lens[16,30,31,35] and do not affect βB1 stability against thermal aggregation and urea denaturation.[29,36] In this research, we investigated the roles of the N-terminal extension of βB1 in protein folding. We found that truncations up to 50 residues off the N-terminus did not affect βB1 stability but significantly affected the kinetic partitioning between the folding and misfolding pathways during βB1 refolding from the denatured state. Our observations strongly suggested that the N-terminal extension of βB1 might act as an intramolecular chaperone (IMC) to facilitate the correct folding and avoid the misfolding/aggregation pathway (Figure 8). From the dissimilarities in the behaviors of various truncated mutants, the key IMC regions could be assigned for the self-refolding of βB1 (residues 17−28) and βA3/βB1 (residues 1−28) as well as the cooperation with αA (residues 17−41). Thus, the segment between residues 17 and 28 was the most important, while the whole N-terminal extension was essential to achieve successful refolding for both homomers and heteromers (Figure 8A).

Distinct from the well-known molecular chaperone, IMC is a specific region within a polypeptide to assist the folding and assembly of the corresponding protein.[49] The bulk of IMCs are identified to be the propeptides usually located at the N- or C-terminus of the preproproteins,[49,50] while several uncleaved regions have also been identified to be IMCs recently.[51−57] There are two types of IMCs: type I is located at the N-terminus and catalyzes the folding reaction, while type II is usually located at the C-terminus and assists the assembly of the quaternary structure.[49] On the basis of our results and those in the literature, the long N-terminal extension of βB1 seems to possess the properties of both type I and type II IMCs: (i) avoidance of the misfolding/aggregation of the homomers (Figure 4); (ii) facilitation of the corefolding of the heteromers (Figure 6); (iii) cooperation with the action of molecular chaperones (Figure 6); (iv) little or no contributions to the stability of both homomers and heteromers (Figure 3 and[29,36]); (v) regulation of the size distribution of homomers and heteromers both in vitro (Figure 2) and in vivo;[16] (vi) existence of both uncleaved and various truncated forms in vivo.[16,30,31,35] Thus, it seems that the N-terminal extension of βB1 is evolved to play diverse functions of IMCs to facilitate the correct folding and assembly of β-crystallins in the highly crowded human lens. At present, it is unclear whether the other members in the β/γ-crystallin family also possess a segment with the IMC function. Considering that βB1 is the most efficient one to fold correctly during kinetic refolding,[23,58,59] the IMC function of βB1 N-terminal extension might be the strongest even if the other members possess an IMC region.

There are two possible mechanisms for the IMC action of βB1 N-terminal extension. One is via the weak binding of the N-terminal extension with the main body of βB1 to stabilize the native state, while the other is through the binding of the N-terminal extension with the exposed hydrophobic interior of the intermediate to avoid misfolding. The weak binding

dx.doi.org/10.1021/bi500146d | Biochemistry 2014, 53, 2464−2473

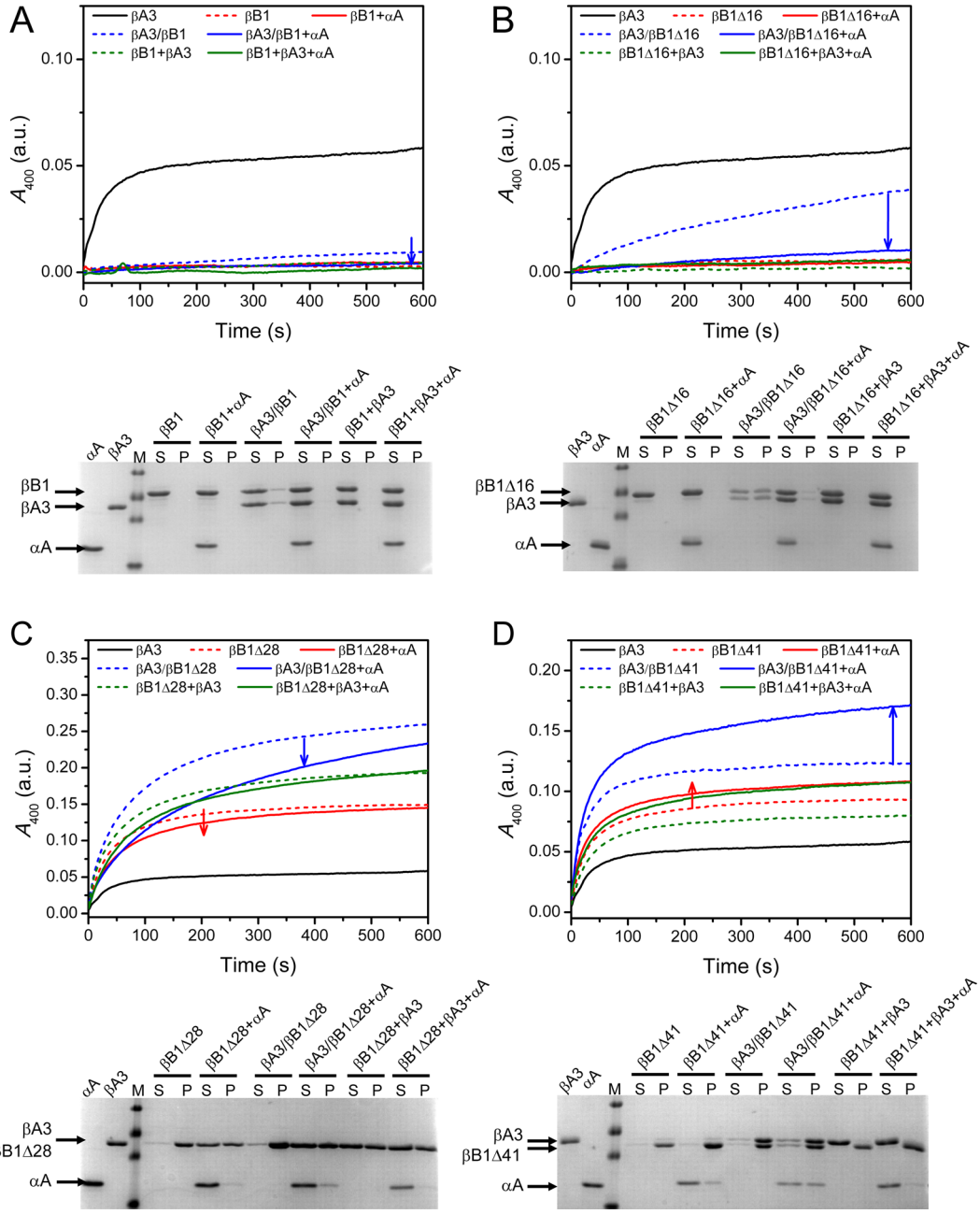

Figure 6. Effect of αA on the partitioning between folding and misfolding/aggregation pathways of βB1 and βA3/βB1 during kinetic refolding. (A) βB1, (B) βB1Δ16, (C) βB1Δ28, (D) βB1Δ41. The experimental conditions were the same as those described in Figure 4 except that the homomers or heteromers were refolded in the presence or absence of an equal molar amount of βA3 or αA. βB1Δ28 has a molecular weight similar to βA3, and thus these two proteins are undistinguishable when analyzed by SDS-PAGE. The behavior of βB1Δ47 and βB1Δ50 was the same as that of βB1Δ41 (data not shown). Top panel: aggregation kinetics measured by turbidity. Bottom panel: SDS analysis of the supernatant (S) and precipitation (P) fractions of samples refolded for 60 min. The label βB1 + βA3 or βB1 + αA represents the refolding of βB1 in buffers in the presence of native βA3 or αA, while βA3/βB1 is the refolding of the heteromer (co-refolding). The changes of βB1 and βA3/βB1 aggregation induced by the addition of αA are indicated by red and blue arrows, respectively.

between the N-terminal extension and βB1 main body has been proposed from the biophysical results in the literature.[26,27] It seems that the N-terminal extension possesses sites of homomer stabilization since the effect of truncations on quaternary structure was much greater than that on secondary or tertiary structures (Figure 2). The binding of the N-terminal extension with extra sites in the intermediate state could not be proved directly. Indirect evidence could be obtained from the fact that heteromers could be formed after the equilibration of the native βB1 truncated forms and βA3 (Figure 2D), whereas the truncated forms of βB1 could not assist βA3 during co-refolding (Figure 5A). Moreover, a longer IMC region was required for βA3/βB1 refolding when compared to βB1 homomer, although this IMC region is not essential for the formation of heteromers. These observations suggested that the N-terminal extension of βB1 might interact with extra sites, which were exposed in the intermediates but got buried in the native state of βB1 and βA3/βB1. Actually, the N-terminal extension of βB1 is a Pro/Ala-rich region and thus has the potency to bind with the intermediate via hydrophobic

dx.doi.org/10.1021/bi500146d | Biochemistry 2014, 53, 2464−2473

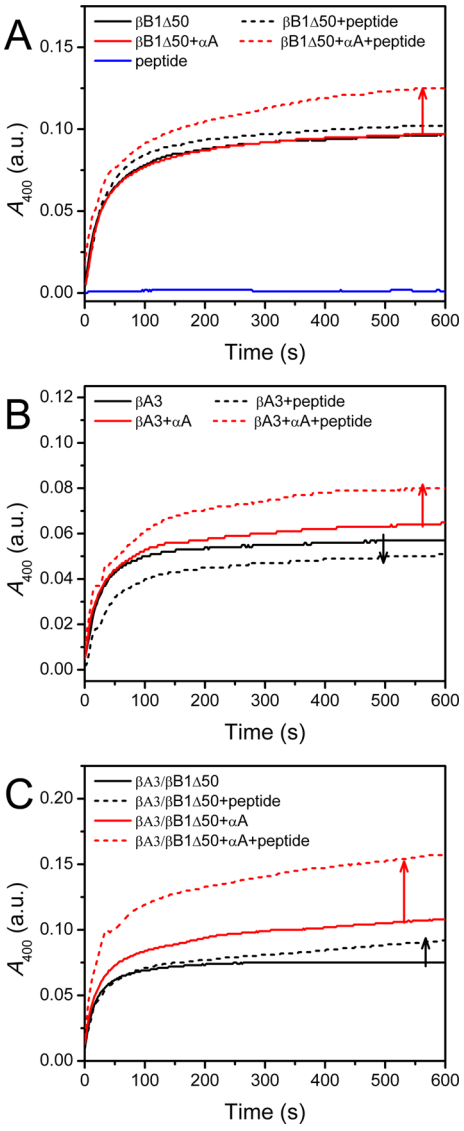

Figure 7. Effect of the synthetic peptide corresponding to the first 50 residues of βB1 on the aggregation of βB1Δ50 (A), βA3 (B), and βA3/βB1Δ50 (C) during kinetic refolding in the presence or absence of αA. The molar ratio between the proteins and the synthetic peptide was 1:60. The experimental conditions were the same as those described in Figure 4A.

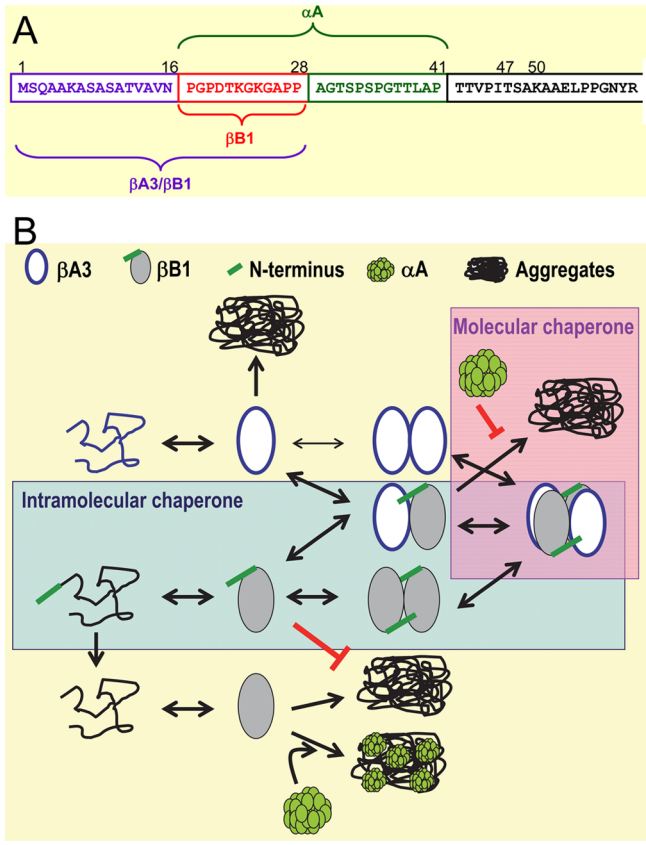

Figure 8. Working models of the IMC functions of the N-terminal extension of βB1. (A) A summary of the key IMC regions required for the self-refolding of β-crystallins and the cooperation with αA. (B) A proposed working model of the combined action of the N-terminal extension of βB1 (intramolecular chaperone) and αA (molecular chaperone). The IMC function of the intact N-terminal extension catalyzes the correct folding of βB1 during kinetic refolding. N-terminal truncations disrupt the IMC function, and the truncated βB1 is more prone to undergo the misfolding/aggregation pathway. βB1 can assist the aggregation-prone βA3 during corefolding, and the combined actions of IMC and molecular chaperone αA facilitate the correct folding of βA3/βB1 heteromer. The disruption of the IMC function of βB1 N-terminal extension retards the folding and releasing processes of αA-trapped β-crystallins and αA is codeposited with the truncated β-crystallins in the precipitation.

interactions and thus enclose the hydrophobic exposure of the intermediate. A similar mechanism also has been revealed for IMC in preproproteins.[50] Interestingly, a recent report has shown that the Pro-rich domain is important to the chaperone function of AIPL1.[60] The key region for the cooperation with αA is also Pro-rich, while the flanked region at the N-terminus is not (Figure 8A). Thus, it is also possible that the N-terminal extension share a similar mechanism when cooperated with molecular chaperones. However, at present it is difficult to distinguish which mechanism dominates the IMC action of βB1 N-terminal extension since the binding of the N-terminal extension with the main body or intermediate should be weak or transient to facilitate the releasing process, similar to the other identified IMCs.[49,50] Further research is necessary to elucidate the underlying mechanism.

The N-terminal extension is not only critical to the avoidance of the misfolding/aggregation pathway of βB1 and βA3/βB1 but also to the function of the lens-specific molecular chaperone αA. The combined action was much more effective than the individual functions of the N-terminal extension and αA. The N-terminal extension could assist the action of αA via binding with αA directly or facilitating βB1 folding after captured by αA. Both mechanisms seem to play a role since all the truncated mutants could be captured by αA, and the key regions were found to be partially overlapping but distinct for β-crystallin self-refolding and refolding assisted by αA. The partially overlapping but distinct key IMC regions provided the basis of the amplification of the chaperone functions through cooperation between IMC and αA. The key to determine a good or bad substrate is whether the αA-bound molecules could be refolded and released or not. The aggregation of βA3/βB1 and βA3/βB1Δ16 could be fully suppressed by equal molar amounts of αA (Figure 6A,B). The existence of part of the N-terminal extension in βB1Δ28 or βA3/βB1Δ28 also facilitated the action of αA, although the partial region had very limited IMC functions. For truncations ≥28 residues, αA was

dx.doi.org/10.1021/bi500146d | *Biochemistry* 2014, 53, 2464−2473

codeposited with the truncated homomers or heteromers. These observations suggested that the hydrophobicity of the intermediate determined the recognition by αA, while the N-terminal extension facilitated the refolding, assembly, and release of β-crystallins. The mutants with intact IMC region could accomplish the correct folding via the help of the N-terminal extension and be released from αA thereafter, while those without the IMC region could not be released and coaggregate with αA (Figure 8B).

In summary, our results indicated that the N-terminal extension acted as an IMC to facilitate the correct folding of βB1 or βA3/βB1. The most interesting finding was that IMC could cooperate with molecular chaperones in protein quality control. In the lens, various crystallins are produced in considerably high concentrations. The combined action of IMCs and molecular chaperones provide an effective mechanism to ensure crystallins to achieve their native structures and to minimize the possibility of the misfolding/aggregation pathway. Thus, our findings provide a novel mechanism to understand the functions of the conserved long N-terminal extension of βB1 and the folding mechanism of crystallins in the lens. Our observations also support the idea proposed recently that the flexible termini of proteins are key players in regulating protein folding and functions.[61] To our knowledge, this is the first report to characterize the cooperation between IMCs and molecular chaperones, which might be important to the understanding of the intracellular quality control mechanisms.

AUTHOR INFORMATION

Corresponding Author

*Tel: +86-10-6278-3477; fax: +86-10-6277-2245; e-mail: ybyan@tsinghua.edu.cn.

Author Contributions

#X.-Y.L. and S.W. made equal contributions.

Funding

This study was partially supported by the National Key Basic Research and Development Program of China (Nos. 2012CB917304 and 2010CB912402).

Notes

The authors declare no competing financial interest.

ACKNOWLEDGMENTS

The authors thank Yi-Bo Xi and Qi-Wei Wang for help with the purification of αA-crystallin.

ABBREVIATIONS

ANS, 1-anilinonaphtalene-8-sulfonate; CD, circular dichroism; DTT, dithiothreitol; E_{max}, emission maximum wavelength of intrinsic fluorescence; GdnHCl, guanidine hydrochloride; IMC, intramolecular chaperone; IPTG, isopropyl-1-thio-β-D-galacto-pyranoside; SDS, sodium dodecyl sulfate; SEC, size-exclusion chromatography; WT, wild type

REFERENCES

(1) Bassnett, S. (2009) On the mechanism of organelle degradation in the vertebrate lens. *Exp. Eye Res. 88*, 133−139.

(2) Andley, U. P. (2007) Crystallins in the eye: function and pathology. *Prog. Retinal Eye Res. 26*, 78−98.

(3) Bloemendal, H., de Jong, W., Jaenicke, R., Lubsen, N. H., Slingsby, C., and Tardieu, A. (2004) Ageing and vision: structure, stability and function of lens crystallins. *Prog. Biophys. Mol. Biol. 86*, 407−485.

(4) Sharma, K. K., and Santhoshkumar, P. (2009) Lens aging: Effects of crystallins. *Biochim. Biophys. Acta 1790*, 1095−1108.

(5) Delaye, M., and Tardieu, A. (1983) Short-range order of crystallin proteins accounts for eye lens transparency. *Nature 302*, 415−417.

(6) Benedek, G. B. (1971) Theory of transparency of the eye. *Appl. Opt. 10*, 459−473.

(7) Benedek, G. B. (1997) Cataract as a protein condensation disease: the Proctor Lecture. *Invest. Ophthalmol. Vis. Sci. 38*, 1911−1921.

(8) Moreau, K. L., and King, J. A. (2012) Protein misfolding and aggregation in cataract disease and prospects for prevention. *Trends Mol. Med. 18*, 273−282.

(9) Shiels, A., Bennett, T. M., and Hejtmancik, J. F. (2010) Cat-Map: putting cataract on the map. *Mol. Vis. 16*, 2007−2015.

(10) Chan, M. P., Dolinska, M., Sergeev, Y. V., Wingfield, P. T., and Hejtmancik, J. F. (2008) Association properties of βB1- and βA3-crystallins: ability to form heterotetramers. *Biochemistry 47*, 11062−11069.

(11) Slingsby, C., and Bateman, O. A. (1990) Quaternary interactions in eye lens beta-crystallins: basic and acidic subunits of β-crystallins favor heterologous association. *Biochemistry 29*, 6592−6599.

(12) Berbers, G. A., Hoekman, W. A., Bloemendal, H., de Jong, W. W., Kleinschmidt, T., and Braunitzer, G. (1983) Proline- and alanine-rich N-terminal extension of the basic bovine β-crystallin B_1 chains. *FEBS Lett. 161*, 225−229.

(13) Lapatto, R., Nalini, V., Bax, B., Driessen, H., Lindley, P. F., Blundell, T. L., and Slingsby, C. (1991) High resolution structure of an oligomeric eye lens beta-crystallin. Loops, arches, linkers and interfaces in beta B2 dimer compared to a monomeric gamma-crystallin. *J. Mol. Biol. 222*, 1067−1083.

(14) Nalini, V., Bax, B., Driessen, H., Moss, D. S., Lindley, P. F., and Slingsby, C. (1994) Close packing of an oligomeric eye lens β-crystallin induces loss of symmetry and ordering of sequence extensions. *J. Mol. Biol. 236*, 1250−1258.

(15) Bax, B., Lapatto, R., Nalini, V., Driessen, H., Lindley, P. F., Mahadevan, D., Blundell, T. L., and Slingsby, C. (1990) X-ray analysis of βB2-crystallin and evolution of oligomeric lens proteins. *Nature 347*, 776−780.

(16) Ajaz, M. S., Ma, Z., Smith, D. L., and Smith, J. B. (1997) Size of human lens β-crystallin aggregates are distinguished by N-terminal truncation of βB1. *J. Biol. Chem. 272*, 11250−11255.

(17) Sergeev, Y. V., David, L. L., Chen, H. C., Hope, J. N., and Hejtmancik, J. F. (1998) Local microdomain structure in the terminal extensions of betaA3- and betaB2-crystallins. *Mol. Vis. 4*, 9.

(18) Montfort, R. L. M. v., Bateman, O. A., Lubsen, N. H., and Slingsby, C. (2003) Crystal structure of truncated human βB1-crystallin. *Protein Sci. 12*, 2606−2612.

(19) Bateman, O. A., Sarra, R., van Genesen, S. T., Kapp, G., Lubsen, N. H., and Slingsby, C. (2003) The stability of human acidic β-crystallin oligomers and hetero-oligomers. *Exp. Eye Res. 77*, 409−422.

(20) Hejtmancik, J. F., Wingfield, P. T., and Sergeev, Y. V. (2004) Beta-crystallin association. *Exp. Eye Res. 79*, 377−383.

(21) Sergeev, Y. V., Hejtmancik, J. F., and Wingfield, P. T. (2004) Energetics of domain-domain interactions and entropy driven association of β-crystallins. *Biochemistry 43*, 415−424.

(22) Pande, A., Pande, J., Ogun, O., Lubsen, N. H., and Benedek, G. B. (2005) Oligomerization and phase transitions in aqueous solutions of native and truncated human βB1-crystallin. *Biochemistry 44*, 1316−1328.

(23) Wang, S., Leng, X.-Y., and Yan, Y.-B. (2011) The benefits of being β-crystallin heteromers: βB1-crystallin protects βA3-crystallin against aggregation during co-refolding. *Biochemistry 50*, 10451−10461.

(24) Cooper, P. G., Carver, J. A., and Truscott, R. J. W. (1993) ^{1}H-NMR spectroscopy of bovine lens βB2-crystallin. *Eur. J. Biochem. 213*, 321−328.
(25) Kroone, R. C., Elliott, G. S., Ferszt, A., Slingsby, C., Lubsen, N. H., and Schoenmakers, J. G. (1994) The role of the sequence extensions in β-crystallin assembly. *Protein Eng. 7*, 1395−1399.
(26) Dolinska, M. B., Sergeev, Y. V., Chan, M. P., Palmer, I., and Wingfield, P. T. (2009) N-terminal extension of βB1-crystallin: identification of a critical region that modulates protein interaction with βA3-crystallin. *Biochemistry 48*, 9684−9695.
(27) Srivastava, K., Gupta, R., Chaves, J. M., and Srivastava, O. P. (2009) Truncated human βB1-crystallin shows altered structural properties and interaction with human βA3-crystallin. *Biochemistry 48*, 7179−7189.
(28) Bateman, O. A., Lubsen, N. H., and Slingsby, C. (2001) Association behaviour of human βB1-crystallin and its truncated forms. *Exp. Eye Res. 73*, 321−331.
(29) Lampi, K. J., Kim, Y. H., Bachinger, H. P., Boswell, B. A., Lindner, R. A., Carver, J. A., Shearer, T. R., David, L. L., and Kapfer, D. M. (2002) Decreased heat stability and increased chaperone requirement of modified human βB1-crystallins. *Mol. Vis. 8*, 359−366.
(30) Lampi, K. J., Ma, Z., Hanson, S. R. A., Azuma, M., Shih, M., Shearer, T. R., Smith, D. L., Smith, J. B., and David, L. L. (1998) Age-related changes in human lens crystallins identified by two-dimensional electrophoresis and mass spectrometry. *Exp. Eye Res. 67*, 31−43.
(31) Ma, Z., Hanson, S. R. A., Lampi, K. J., David, L. L., Smith, D. L., and Smith, J. B. (1998) Age-related changes in human lens crystallins identified by HPLC and mass spectrometry. *Exp. Eye Res. 67*, 21−30.
(32) Santhoshkumar, P., Udupa, P., Murugesan, R., and Sharma, K. K. (2008) Significance of interactions of low molecular weight crystallin fragments in lens aging and cataract formation. *J. Biol. Chem. 283*, 8477−8485.
(33) Su, S. P., McArthur, J. D., and Andrew Aquilina, J. (2010) Localization of low molecular weight crystallin peptides in the aging human lens using a MALDI mass spectrometry imaging approach. *Exp. Eye Res. 91*, 97−103.
(34) Wang, S., Zhao, W.-J., Liu, H., Gong, H., and Yan, Y.-B. (2013) Increasing βB1-crystallin sensitivity to proteolysis caused by the congenital cataract-microcornea syndrome mutation S129R. *Biochim. Biophys. Acta, Mol. Basis Dis. 1832*, 302−311.
(35) David, L. L., Lampi, K. J., Lund, A. L., and Smith, J. B. (1996) The sequence of human βB1-crystallin cDNA allows mass spectrometric detection of βB1 protein missing portions of its N-terminal extension. *J. Biol. Chem. 271*, 4273−4279.
(36) Kim, Y. H., Kapfer, D. M., Boekhorst, J., Lubsen, N. H., Bachinger, H. P., Shearer, T. R., David, L. L., Feix, J. B., and Lampi, K. J. (2002) Deamidation, but not truncation, decreases the urea stability of a lens structural protein, βB1-crystallin. *Biochemistry 41*, 14076−14084.
(37) Pang, M., Su, J.-T., Feng, S., Tang, Z.-W., Gu, F., Zhang, M., Ma, X., and Yan, Y.-B. (2010) Effects of congenital cataract mutation R116H on αA-crystallin structure, function and stability. *Biochim. Biophys. Acta, Proteins Proteomics 1804*, 948−956.
(38) Wang, K. J., Wang, S., Cao, N.-Q., Yan, Y.-B., and Zhu, S. Q. (2011) A novel mutation in *CRYBB1* associated with congenital cataract-microcornea syndrome: the p.Ser129Arg mutation destabilizes the βB1/βA3-crystallin heteromer but not the βB1-crystallin homomer. *Hum. Mutat. 32*, E2050−E2060.
(39) Sun, T.-X., Das, B. K., and Liang, J. J. N. (1997) Conformational and functional differences between recombinant human lens αA- and αB-crystallin. *J. Biol. Chem. 272*, 6220−6225.
(40) Bradford, M. M. (1976) A rapid and sensitive method for the quantitation of microgram quantities of protein utilizing the principle of protein-dye binding. *Anal. Biochem. 72*, 248−254.
(41) Turoverov, K. K., Haitlina, S. Y., and Pinaev, G. P. (1976) Ultraviolet fluorescence of actin. Determination of native actin content in actin preparations. *FEBS Lett. 62*, 4−6.
(42) He, G.-J., Zhang, A., Liu, W.-F., Cheng, Y., and Yan, Y.-B. (2009) Conformational stability and multistate unfolding of poly(A)-specific ribonuclease. *FEBS J. 276*, 2849−2860.
(43) Jiang, Y., Yan, Y.-B., and Zhou, H.-M. (2006) Polyvinylpyrrolidone 40 assists the refolding of bovine carbonic anhydrase B by accelerating the refolding of the first molten globule intermediate. *J. Biol. Chem. 281*, 9058−9065.
(44) Lampi, K. J., Oxford, J. T., Bachinger, H. P., Shearer, T. R., David, L. L., and Kapfer, D. M. (2001) Deamidation of human βB1 alters the elongated structure of the dimer. *Exp. Eye Res. 72*, 279−288.
(45) Kurganov, B. I. (2002) Kinetics of protein aggregation. Quantitative estimation of the chaperone-like activity in test-systems based on suppression of protein aggregation. *Biochemistry (Moscow) 67*, 409−422.
(46) He, G.-J., Liu, W.-F., and Yan, Y.-B. (2011) Dissimilar roles of the four conserved acidic residues in the thermal stability of poly(A)-specific ribonuclease. *Int. J. Mol. Sci. 12*, 2901−2916.
(47) Horwitz, J. (1992) α-Crystallin can function as a molecular chaperone. *Proc. Natl. Acad. Sci. U. S. A. 89*, 10449−10453.
(48) Slingsby, C., and Clout, N. J. (1999) Structure of the crystallins. *Eye (London) 13*, 395−402.
(49) Chen, Y. J., and Inouye, M. (2008) The intramolecular chaperone-mediated protein folding. *Curr. Opin. Struct. Biol. 18*, 765−770.
(50) Schulz, E. C., Dickmanns, A., Urlaub, H., Schmitt, A., Muhlenhoff, M., Stummeyer, K., Schwarzer, D., Gerardy-Schahn, R., and Ficner, R. (2010) Crystal structure of an intramolecular chaperone mediating triple-beta-helix folding. *Nat. Struct. Mol. Biol. 17*, 210−215.
(51) Markossian, K. A., Golub, N. V., Khanova, H. A., Levitsky, D. I., Poliansky, N. B., Muranov, K. O., and Kurganov, B. I. (2008) Mechanism of thermal aggregation of yeast alcohol dehydrogenase I: role of intramolecular chaperone. *Biochim. Biophys. Acta, Proteins Proteomics 1784*, 1286−1293.
(52) Liu, W.-F., Zhang, A., He, G.-J., and Yan, Y.-B. (2007) The R3H domain stabilizes poly(A)-specific ribonuclease by stabilizing the RRM domain. *Biochem. Biophys. Res. Commun. 360*, 846−851.
(53) He, H.-W., Feng, S., Pang, M., Zhou, H.-M., and Yan, Y.-B. (2007) Role of the linker between the N- and C-terminal domains in the stability and folding of rabbit muscle creatine kinase. *Int. J. Biochem. Cell Biol. 39*, 1816−1827.
(54) Brunger, A. T., Breidenbach, M. A., Jin, R., Fischer, A., Santos, J. S., and Montal, M. (2007) Botulinum neurotoxin heavy chain belt as an intramolecular chaperone for the light chain. *PLoS Pathog. 3*, 1191−1194.
(55) Bhattacharyya, J., Santhoshkumar, P., and Sharma, K. K. (2003) A peptide sequence-YSGVCHTDLHAWHGDWPLPVK [40−60]-in yeast alcohol dehydrogenase prevents the aggregation of denatured substrate proteins. *Biochem. Biophys. Res. Commun. 307*, 1−7.
(56) Ma, B., Tsai, C. J., and Nussinov, R. (2000) Binding and folding: in search of intramolecular chaperone-like building block fragments. *Protein Eng. 13*, 617−627.
(57) Chen, Z., Chen, X.-J., Xia, M., He, H.-W., Wang, S., Liu, H., Gong, H., and Yan, Y.-B. (2012) Chaperone-like effect of the linker on the isolated C-terminal domain of rabbit muscle creatine kinase. *Biophys. J. 103*, 558−566.
(58) Zhang, W., Cai, H.-C., Li, F.-F., Xi, Y.-B., Ma, X., and Yan, Y.-B. (2011) The congenital cataract-linked G61C mutation destabilizes γD-crystallin and promotes non-native aggregation. *PLoS One 6*, e20564.
(59) Xu, J., Wang, S., Zhao, W.-J., Xi, Y.-B., Yan, Y.-B., and Yao, K. (2012) The congenital cataract-linked A2V mutation impairs tetramer formation and promotes aggregation of βB2-crystallin. *PLoS One 7*, e51200.
(60) Li, J., Zoldak, G., Kriehuber, T., Soroka, J., Schmid, F. X., Richter, K., and Buchner, J. (2013) Unique proline-rich domain regulates the chaperone function of AIPL1. *Biochemistry 52*, 2089−2096.
(61) Uversky, V. N. (2013) The most important thing is the tail: Multitudinous functionalities of intrinsically disordered protein termini. *FEBS Lett. 587*, 1891−1901.